Proceedings of the ASME 2010 3rd Joint US-European Fluids Engineering Summer Meeting and 8th International Conference on Nanochannels, Microchannels, and Minichannels
FEDSM-ICNMM2010
August 1-5, 2010, Montreal, Canada

FEDSM-ICNMM2010-30437

CONTROL OF FLOW ASYMMETRY AROUND SLENDER BODY OF REVOLUTION AT HIGH INCIDENCE WITH MINUTE JETS

Xiaorong Guan
School of Aerospace, Tsinghua University
Beijing, China

Cheng Xu
School of Mechanical Engineering,
Nanjing University of Science and Technology
Nanjing, Jiangsu, China

ABSTRACT

For controlling the flow asymmetry around slender body of revolution at high incidence, a method with skew minute jets distributed symmetrically on opposite sides before separation lines near nose apex is put forward and numerically confirmed. By configuring the jet primary parameters, an active control can be achieved along with the intensity and location variations of the concentrated vortices originated from the interaction between the jets and the flow around slender body. The control effect is realized through the regulation of the concentrated vortices on the asymmetry degree of nose vortices near nose apex. In order to achieve effective control, several rules on configuring the jet primary parameters should be followed: the concentrated vortices are intensive sufficiently and close enough to nose vortices; the concentrated vortices can keep acting on nose vortices in an adequately long axial extent.

Slender body of revolution; High-incidence aerodynamics; Asymmetric vortical flow; Minute jet; Flow control

INTRODUCTION

The flow around slender body of revolution at incidence has been studied extensively [1-16]. It has been affirmed that the flow in high incidence range usually appears in Asymmetric Vortical Pattern (abbr., AVP) and induces remarkable side force and yawing moment on the body even under the zero sideslip condition. Owing to the lateral characteristics, the control of the flow has become one of the most significant objects in the field of aerodynamics research. Since the vortical flow is influenced by lots of factors (such as incidence, freestream Mach number, Reynolds number, etc) [5-12] together, its structure and aerodynamic characteristics are changeful. Especially, the vortical flow is highly sensitive to the minute perturbations near nose apex (such as the unavoidable minute imperfections produced in model machining) [7-9], and it is just about the size and distribution randomness of nose perturbation that results in the difficulty in exactly predicting the flow.

To this day, the origin of the flow asymmetry hasn't been cleared completely. At present, there are two primary viewpoints coexisting. One considers that the flow asymmetry is realized through the boundary-layer viscosity [4,14,15], while the other considers that the flow asymmetry is realized through the flow instability [9,10,16]. In the viscosity viewpoint, the asymmetry of the vortical structure is induced by the asymmetry of boundary-layer transition, separation. While in the instability viewpoint, the asymmetry of boundary layer transition, separation is not a necessary condition to the formation of the asymmetry of the vortical structure, and it might be a result of the asymmetry of the vortical structure instead. This shows that the consequence of these two viewpoints is just converse. In fact, the asymmetry of both vortical structure and boundary-layer transition, separation usually coexists, so it is difficult to tell the consequence. However, the instability viewpoint has obtained more support recently.

Nevertheless, based on the researcher's own understanding on the origin of the asymmetry, many control methods have been developed and different effects have been achieved [10,17-25]. The control methods can be classified into two types: passive and active. The passive method is adopted to restrain or eliminate the flow asymmetry. The passive control is usually carried out through directly modifying nose shape, improving surface quality near nose apex [17,18], or appending auxiliary equipments (such as strakes, etc.) [19,20]. All of them have certain control abilities, but can just take effect under special conditions and can't adjust to the flow change.

The active method is more aspiring. It is usually used to regulate the asymmetry with aerodynamic actuators [21]. By commanding their on-off and adjusting their effect intension, the flows of different asymmetry degrees can be achieved. At present, as active methods, nose-blowing [10,22,23] and actuated-forebody-strake [24,25] are studied and applied widely. All of them have certain control effect in model and even flight experiments, but none of them has been applied to engineering practice.

On the background and based on the instability viewpoint, a new active method with skew minute jets is advanced here to control the flow asymmetry around slender body of revolution at high incidence. By analyzing the influence of jet primary parameters on the control effect, the control mechanism and several rules on optimizing the configuration of these parameters have been explored as well.

NOMENCLATURE

C_p	$=\left(p-p_\infty\right)\Big/q$, surface-pressure coefficient
C_z	$=-\left(\int_0^{2\pi} p(\theta)\sin\theta \mathrm{d}\theta\right)\Big/\left(2q\sin^2\alpha\right)$, sectional-side-force coefficient
$C_{z\mathrm{r}}$	Ratio of total side force with control to without control
D	Diameter of cylindrical afterbody
H_d	$=\left(\nabla\times\boldsymbol{V}\right)\cdot\boldsymbol{V}$, helicity density
M_∞	Freestream Mach number
p, p_∞	Surface pressure, freestream pressure
q	$=\rho_\infty U_\infty^{\ 2}\Big/2$, freestream dynamic pressure
Re_D	$=U_\infty D\sin\alpha\Big/\nu$, Reynolds number
U_∞	Freestream velocity
$\boldsymbol{V}$	Velocity vector
α	Incidence
β	Jet skew angle, i.e., the angle between projections of jet and freestream directions on the plane tangent to jet orifice at the center
θ	Azimuthal angle
λ	Ratio of jet velocity to freestream velocity
ν	Kinematic viscosity
ρ_∞	Freestream density
ω	$=\nabla\times\boldsymbol{V}$, vorticity

THEORETICAL BACKGROUND

Governing Equations and Numerical Algorithms

The conservation equations of mass, moment and energy can be expressed generally in a conservative flux-vector form, which is convenient for numerical computation, i.e.,

$$\partial_\tau\hat{\boldsymbol{Q}}+\partial_\xi(\hat{\boldsymbol{F}}+\hat{\boldsymbol{F}}_\mathrm{v})+\partial_\eta(\hat{\boldsymbol{G}}+\hat{\boldsymbol{G}}_\mathrm{v})+\partial_\varsigma(\hat{\boldsymbol{H}}+\hat{\boldsymbol{H}}_\mathrm{v})=0 \qquad (1)$$

where the variables and flux vectors are explained in Ref. [26].

A control-volume based method is employed to discretize the governing equations. The convection terms are discretized spatially with the MUSCL scheme, which can reduce numerical diffusions; the diffusion terms are discretized spatially with the second-order central-differencing scheme. And the temporal discretization is performed with a second-order fully-implicit scheme, which is unconditionally stable with respect to time-step size.

Turbulence Model

The coefficients of viscosity and thermal conductivity in the governing equations are given independently from auxiliary relations. The coefficients of molecular and turbulent viscosities are respectively obtained from the Sutherland's law and SST k-ω model [27], which is suitable to outer flows and accurate, reliable for both near-wall and far-field flow zones. Then the coefficient of thermal conductivity is obtained as the viscosity coefficient is known by assuming a constant Prandtl number. The discretization schemes adopted here are similar to those for the above governing equations, except that the convection terms are discretized spatially here with a modified QUICK scheme, which can reduce numerical diffusions and is unconditionally stable.

Body Configuration and Computational Grid

The slender body of revolution consists of a 3D-long ogive nose and a 7D-long cylindrical afterbody. They are tangentially jointed. For obtaining a deterministic, remarkably asymmetric baseline flow (i.e., without control), a single minute geometric bump sketched in Fig. 1. is employed to act as nose perturbation [7].

The control system consists of three pairs of minute jet orifices (L1/R1, L2/R2 and L3/R3, sketched in Fig. 2.), and the diameters are 0.003D uniformly. They are almost distributed circumferentially before the separation lines on both sides [12], which is distinct from the previous blowing methods [28,29].

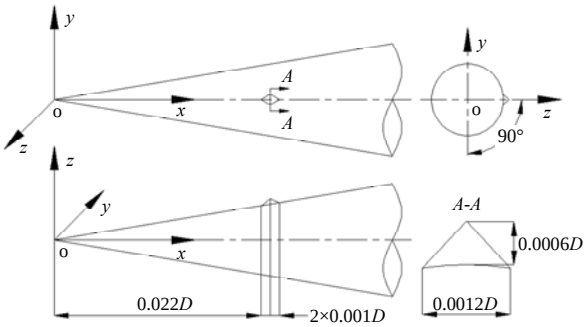

FIGURE 1. SKETCH OF MINUTE GEOMETRIC BUMP AND COORDINATE SYSTEM FOR DATA PROCESSING.

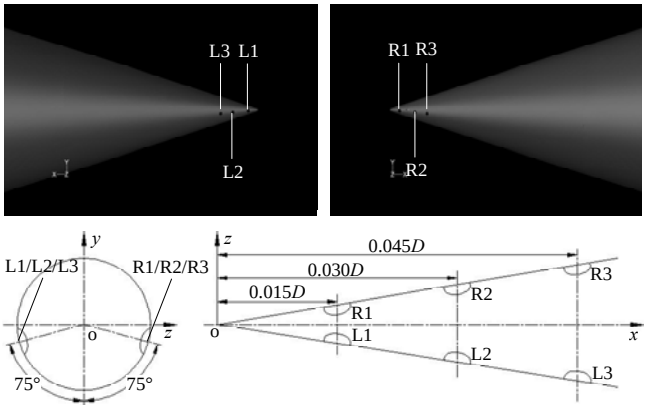

FIGURE 2. SPATIAL DISTRIBUTION OF JET ORIFICES.

The computational outer boundary extends 12D radially from the body surface and 10D axially in front of the body. The computational grid is kept symmetric with respect to the fore-and-aft symmetric plane of the model, except in a weeny zone near the bump. The grid extending completely about the model consists of 130 circumferential planes. In each circumferential plane, the grid contains 60 radial points between body surface and computational outer boundary, and 100 axial points between nose apex and model rear. The circumferential grid planes are clustered properly in leeside of the model to resolve the vortices. The radial grid points are clustered properly near body surface to resolve the viscous layer. The minimal radial grid spacing is fixed at 0.00001D to assure a value of y^+<5 near body surface, and to have at least 20 radial grid points within the viscous layer. The grid points are also clustered properly near jet orifices to resolve the interaction between the minute jets and the flow around slender body.

Boundary Conditions and Initial Conditions

An adiabatic no-slip condition is maintained at the body surface, which excludes the surfaces of jet orifices. When a jet is turned off, an adiabatic no-slip condition is enforced at its orifice surface; when a jet is turned on, a velocity-inlet condition is applied instead, and the jet

characteristics are supposed to be uniformly distributed on the orifice surface. A characteristic condition is kept at the computational outer boundary: at the upstream, the freestream values are specified; at the downstream, the non-reflected condition is applied [30]. In addition, a periodic continuation condition is enforced at the circumferential grid edges.

When performing the computation of the baseline flow, the entire flowfield is initially set to the freestream condition throughout the grid. When performing the computation of the flow with control, the flowfield is initially set to the baseline case or a case with control obtained previously. A global-constant time step is employed for time-dependent computation, and the solution is marched in time until a quasi-steady flowfield is achieved.

Examinations of Computational Results

It has been validated in Ref. [7] that the numerical methods and the flow models discussed above are suitable to the current study and the computational results are fairly reliable.

COMPUTATIONAL RESULTS AND DISCUSSIONS

All the computations are performed for M_∞=0.2, α=50°, and Re_D=1.4×10^6.

Conventions for Data Processing

The right-handed coordinate system illustrated in Fig. 1. is employed here, where the origin is located at the nose apex of the body, and the x axis is aligned with the principal axis, and the z axis is perpendicular to the plane of the freestream velocity vector. The x and y velocity components of freestream are both positive in the system.

The orientations of "left" and "right" appearing below are defined with respect to plane z=0 when looking along the positive x direction. The "symmetric" and "asymmetric" are also defined with respect to plane z=0. Besides, θ=0° is fixed at the windward sideline of the fore-and-aft symmetric plane of the body, and the positive direction is defined anticlockwise when looking along the positive x direction.

Conventions for Configuring Jet Primary Parameters

For simplifying the control strategy and improving the control maneuverability, several conventions on configuring jet primary parameters are followed here: (1) the jet primary parameters are kept symmetric; (2) the primary parameters of the jets on one side are kept uniform; (3) the pitching angle (i.e., the angle between the directions of jet and its projection on the plane tangent to jet orifice at the center) of all jets is fixed at 30°, which is favorable to flow control [31].

Baseline Flow

It can be known from Ref. [7] that the baseline flow adopted here is remarkably asymmetric. Downstream axially, it presents itself in the structure of leeside vortices forming, rising and shedding alternately from opposite sides of the body, and induces the surface pressure of distributing asymmetrically and the sectional side force of waving sinusoidally (demonstrated in Fig. 3.). For expression convenience, the two leeside vortices originated near nose apex (i.e., V_{L1} and V_{R1}) are named nose vortices here.

Interaction between Minute Jets and the Flow around Slender Body

Under certain jet conditions, concentrated vortices form near the jet orifices due to the interaction between the jets and the flow around slender body (illustrated in Fig. 4). Owing to the "entrainment" of mainstream, such concentrated vortices dissipate quickly downstream. However, they can still take remarkable effect on nose vortices to alter their intensity, position and shape. The effect is influenced by both the relative intensity of concentrated vortex to nose vortex and the distance between them: the more intensive the relative intensity is and/or the shorter the distance is, the stronger the effect is. In cross-section, for the rotational directions of concentrated vortex and the nose vortex on one side are uniform, partial vorticity of the concentrated vortex is convoluted into the nose vortex in the process of the concentrated vortex dissipating. After absorbing vorticity from the concentrated vortex, the nose vortex intensifies more or less.

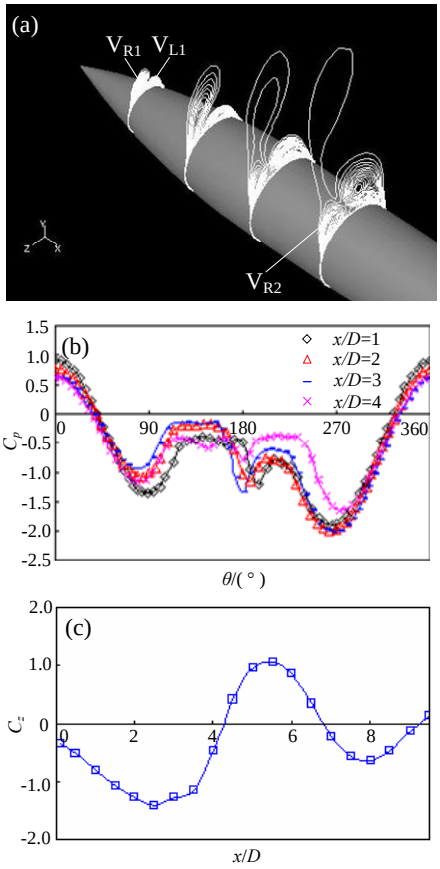

FIGURE 3. BASELINE FLOW: (a) CONTOUR MAPS OF $|H_d|$ [32], (b) CIRCUMFERENTIAL DISTRIBUTIONS OF C_p, (c) AXIAL EVOLUTION OF C_z.

The formation of such concentrated vortices also takes effect on the flow pattern on body surface (illustrated in Fig. **5**). For the concentrated vortices dissipate quickly, their effect on the flow pattern on body surface is almost located only near nose apex of the slender body and the separation lines do not shift obviously (i.e., the boundary-layer separation is not obviously restrained or delayed).

Additionally, the concentrated vortices will take effect on the aerodynamic characteristics near nose apex (demonstrated in Fig. 6.) as well. Near jet orifices, the negative surface pressure decreases obviously. With nose vortices absorbing vorticity from concentrated vortices and intensifying, their inducement on the body surface strengthens, and the negative surface pressure in the vicinity of nose vortices increases.

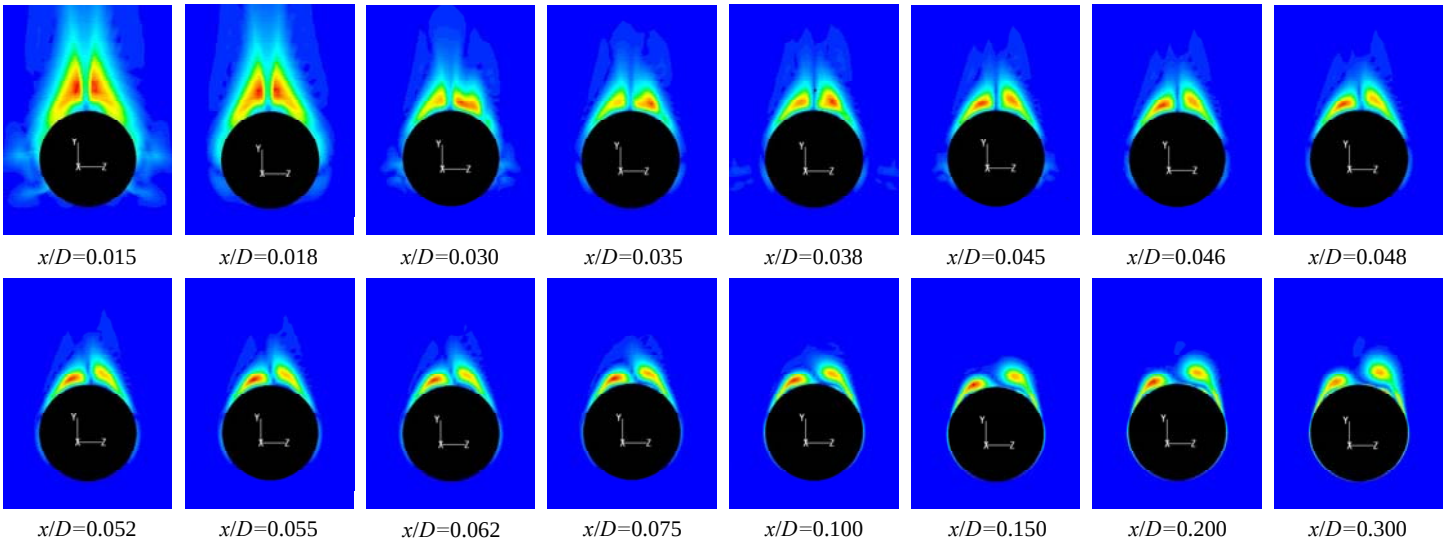

(a)

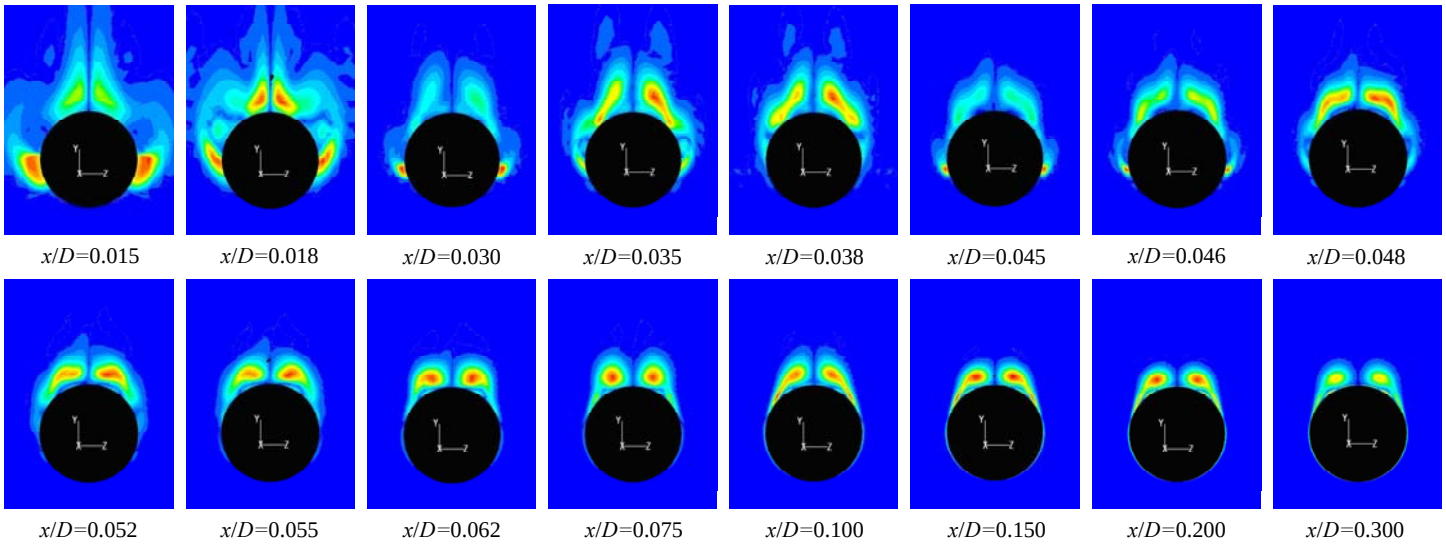

(b)

FIGURE 4. CONTOUR MAPS OF $|H_d|$: (a) BASELINE FLOW, (b) ALL JETS ON, λ=0.90, β=60° (WINDWARD).

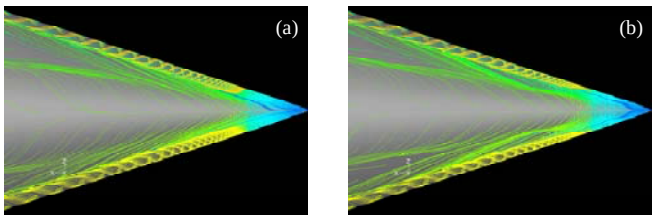

FIGURE 5. FLOW PATTERNS ON BODY SURFACE NEAR NOSE APEX: (a) BASELINE FLOW, (b) All JETS ON, λ=0.90, β=60° (WINDWARD).

Control Effect of Minute Jets on Flow Asymmetry

It can be found that, when the minute jets turned on, the flow asymmetry near nose apex weakens obviously (demonstrated in Fig. 4. and 6.), and the global flow asymmetry also weakens (demonstrated in Fig. 7. to 9.). It indicates that, by setting up such jets near nose apex to form concentrated vortices, the flow asymmetry near nose apex can be weakened obviously and further the objective of weakening the global flow asymmetry can be achieved. This correlation is coincident with the conclusion drawn from Ref. [7] that with the axial extent of Symmetric Vortical Pattern (abbr., SVP) near nose apex elongating from zero gradually, the global flow asymmetry weakens by degrees. Namely, due to the effect of concentrated vortices on nose vortices, the axial location that the nose vortices begin to appear in remarkable AVP is staved downstream, so the global flow asymmetry weakens.

The effect of concentrated vortices on nose vortices near nose apex can be implemented directly or indirectly through concentrated vortices acting on the flow pattern on body surface near nose apex. How on earth do concentrated vortices affect the intensity, shape and position of nose vortices near nose apex and further weaken the flow asymmetry near nose apex?

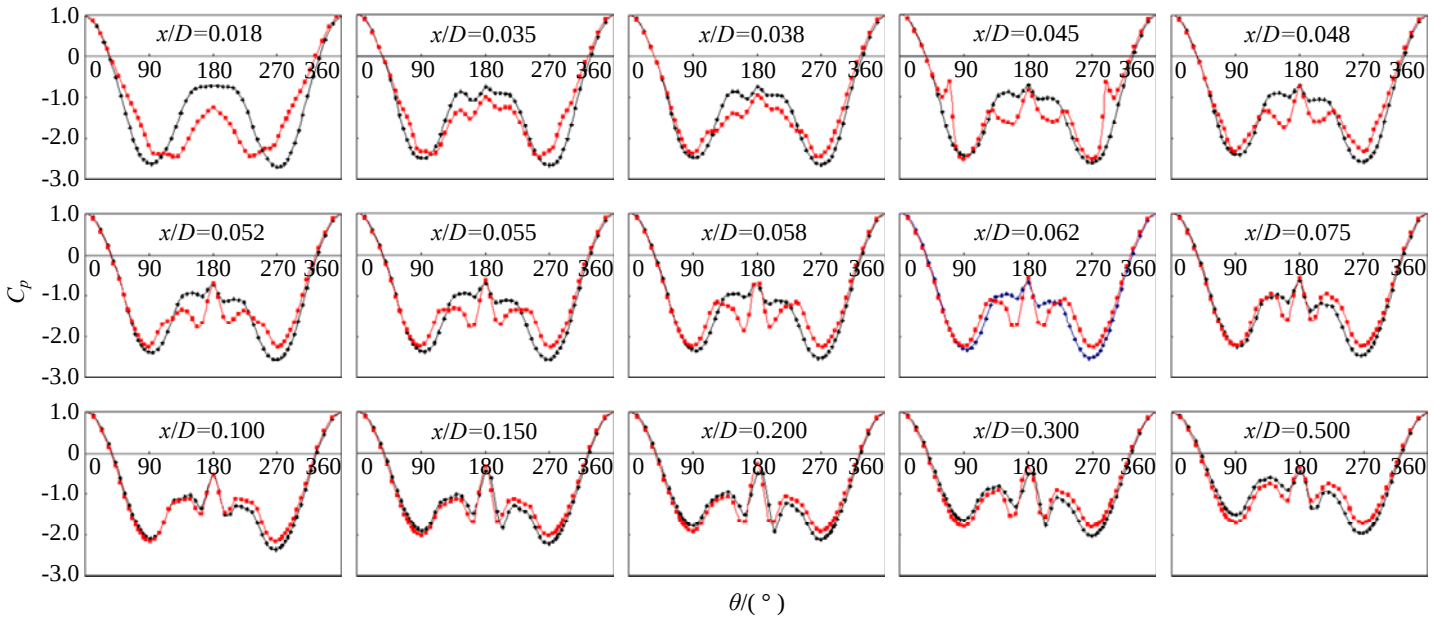

FIGURE 6. CIRCUMFERENTIAL DISTRIBUTIONS OF C_p AT DIFFERENT AXIAL LOCATIONS.

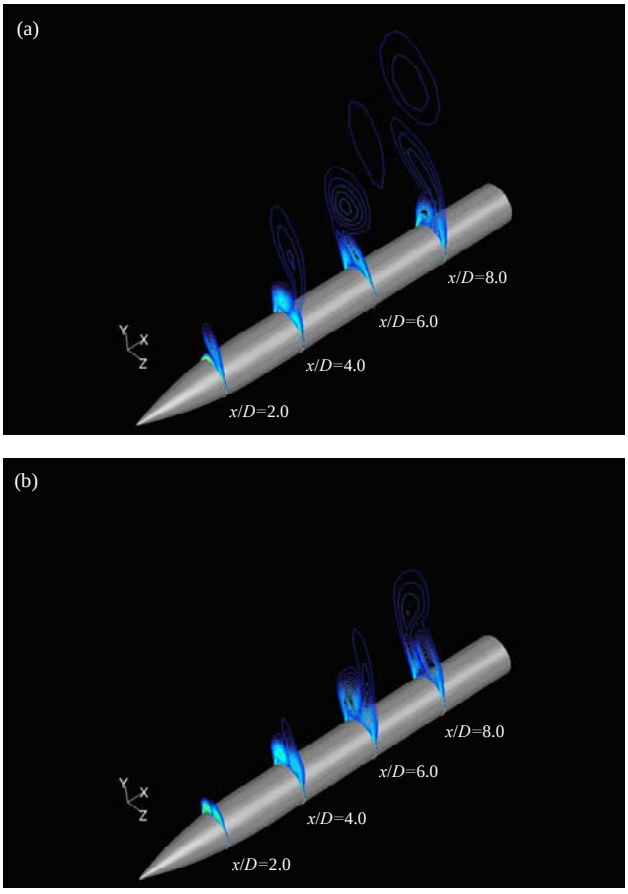

FIGURE 7. CONTOUR MAPS OF $|H_d|$: (a) BASELINE FLOW, (b) ALL JETS ON, λ=0.90, β=60° (WINDWARD).

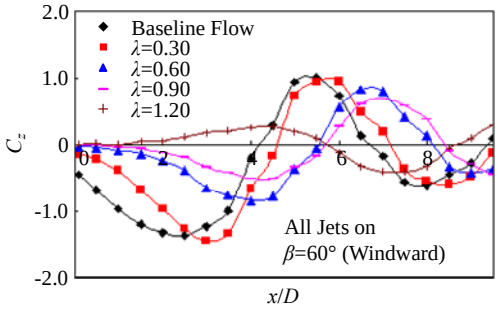

FIGURE 8. AXIAL EVOLUTIONS OF C_z BEFORE AND AFTER JETS TURNED ON.

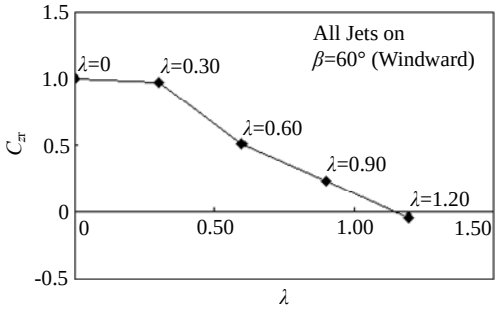

FIGURE 9. VARIATION OF C_{zr} ALONG WITH λ.

The standpoint here is inclined to the direct manner. On obverse side, the direct action of concentrated vortices on nose vortices can be clearly observed (illustrated in Fig. 4. and 6.). On reverse side: (1) the concentrated vortices indeed affect the flow pattern on body surface, but the separation lines shift little (illustrated in Fig. 5); (2) if the concentrated vortices restrain or delay the separation of the boundary layer, compared to the baseline flow, the nose vortices must be smaller and weaker at the same cross section near nose apex, however the

phenomenon observed is just inverse; (3) further if the concentrated vortices restrain or delay the separation of the boundary layer, it is uncertain that the global flow asymmetry around slender body will weaken. According to the conclusion drawn from Ref. [7], it can be obtained that the farther away from nose apex the axial location of obvious asymmetry of nose vortices beginning to appear is, the weaker the global flow asymmetry is. Here, "the farther away from nose apex the axial location of obvious asymmetry of nose vortices beginning to appear is" means that "the longer the distance of nose vortices having developing is downstream axially before the obvious asymmetry appearing", so it can be known that the more intensive and the bigger the nose vortices are before the obvious asymmetry appearing, the weaker the global flow asymmetry is. So even though the separation of boundary layer is restrained or delayed, if the nose vortices turn to asymmetric rapidly after forming, the global flow asymmetry might still be very remarkable. Contrarily, the direct effect of concentrated vortices on nose vortices can enlarge and intensify the nose vortices, and therefore the global flow asymmetry will weaken.

Here, an idea may come out naturally: through configuring the jet primary parameters to adjust the intensity, location of concentrated vortices, the flows of different asymmetry degrees can be obtained (i.e., the active control can be achieved) along with the variation of the effect of concentrated vortices on nose vortices. In fact, the idea has been validated preliminarily in Fig. 8. and 9..

Influence of Jet Primary Parameters on Control Effect

For achieving active control on the flow asymmetry, the influence of jet primary parameters on the control effect should be studied.

Axial Distribution of Jets For a single pair of jets, the farther away from nose apex they are, the weaker their control effect is (illustrated in Fig. 10.). It shows that, when a single pair of jets shifts downstream, the regulation of concentrated vortices on the asymmetry degree of nose vortices weakens (demonstrated in Fig. 4. and 6.).

It can be drawn from Fig. 2. that, with a single pair of jets shifts downstream, their distances away from nose vortices elongate, which means that the concentrated vortices become farther away from nose vortices when forming. Besides, the relative intensity of concentrated vortices to nose vortices weakens, because nose vortices grow more intensive while concentrated vortices almost keep steady. Thus it's easy to understand the influence of jet axial location on the regulation.

Actually, the control effect of a single pair of jets on the global flow asymmetry is always very faint (demonstrated in Fig. 10.). For concentrated vortices dissipate downstream quickly, the axial extent of their regulation on nose vortices is very short. Namely, their regulation can just momently restrain the axial development of flow asymmetry near nose apex, and naturally the control effect on the global flow asymmetry is very faint.

The control effect of two pairs of jets together is based on the respective control effect of each pair of jets in the current combination (demonstrated in Fig. 10.). The concentrated-vortex pairs originated from both jet pairs L1/R1 and L2/R2 can solely restrain the axial evolution of flow asymmetry near nose apex. So when the two pairs of jets are distributed close axially, their concentrated vortices are combined together to restrain the flow asymmetry near nose apex in a certain axial extent, and the axial location of obvious AVP beginning to appear is delayed downstream. Thus the global flow asymmetry is effectively restrained. The control effect of two jet pairs L1/R1, L3/R3 together or L2/R2, L3/R3 together is almost equivalent respectively to that of jet pair L1/R1 solely or L2/R2 solely (demonstrated in Fig. 10.). This is because the control effect of jet pair L3/R3 is too faint and even can be neglected.

The control effect of three pairs of jets together is equal to that of L1/R1, L2/R2 together (demonstrated in Fig. 10.). It is also because that the control effect of jet pair L3/R3 solely can almost be neglected. Namely, the emergence of jet pair L3/R3 doesn't elongate the axial regulation extent of concentrated vortices from both jet pairs L1/R1 and L2/R2 on nose vortices.

Magnitude of Jet Velocity The magnitude of jet velocity has significant influence on the control effect. When the jet-velocity magnitude alters, the intensity, shape and position of the concentrated vortices alter accordingly (demonstrated in Fig. 11.), and further the regulation on nose vortices alters, so naturally the control effect on the global flow asymmetry alters. It can be drawn from Fig. 12. (except the cases of β=0°, which is to be discussed below) that, with jet-velocity magnitude increasing, the control effect of concentrated vortices on the global flow asymmetry strengthens, and the asymmetry even reverses when the magnitude increases to a certain value. Thus it can be seen that the active control can be achieved by just adjusting the jet-velocity magnitude.

For the concentrated vortices originated from jet pairs L1/R1, L2/R2 begin to take effect on nose vortices rapidly just after forming, it is hard to find out the characteristics of the concentrated vortex by analyzing these concentrated vortices. Therefore, the concentrated vortices originated from the jet pair L3/R3 are taken below to discuss the characteristics of the concentrated vortex itself.

Under the condition of different jet-velocity magnitudes, the intensity, shape and position of concentrated vortices are different respectively (demonstrated in Fig. 11.). Thus, their regulation on nose vortices is different (demonstrated in Fig. 13.), and further their control effect on the global flow asymmetry is different accordingly (demonstrated in Fig. 12.). In the current work, with jet-velocity magnitude increasing gradually, the control effect of minute jets on the global flow asymmetry intensifies by degrees. The intensifying of the effect of concentrated vortices on nose vortices is supposed to be responsible for this correlation, which is caused through the following two ways.

(1) With jet-velocity magnitude increasing by degrees, the concentrated vortices intensify by degrees (demonstrated in Fig. 11. and 13.), which leads the regulation of concentrated vortices on nose vortices to strengthen.

(2) With jet-velocity magnitude increasing by degrees, the "entrainment" of minute jets on concentrated vortices strengthens by degrees, which directs away from body surface. Accordingly, the distances between concentrated vortices and body surface increase by degrees (demonstrated in Fig. 11.), and the "entrainment" of mainstream on concentrated vortices strengthens by degrees, which directs leeward, so the distances between concentrated vortices and nose vortices decrease by degrees and then the regulation of concentrated vortices on nose vortices strengthens by degrees.

The impression of the concentrated vortices originated from jet pairs L1/R1 and L2/R2 performing regulation on nose vortices can be observed downstream axially near the orifices of jet pair L3/R3 (demonstrated in Fig. 11. and 13.). With jet-velocity magnitude increasing gradually, the regulation of concentrated vortices originated from jet pairs L1/R1, L2/R2 on nose vortices strengthens by degrees, and accordingly the vorticity convoluted into nose vortices increases by degrees, so naturally the nose vortices intensify and expand by degrees. At the same time, the nose vortices are induced to shift outwards gradually. Therefore, the distances between downstream concentrated vortices and nose vortices decrease further, so the regulation of downstream vortices on nose vortices strengthens further.

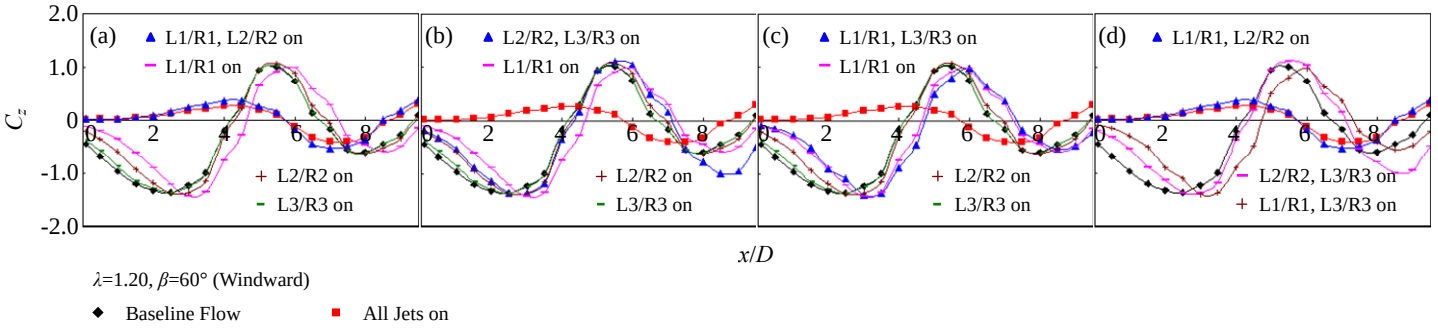

FIGURE 10. INFLUENCE OF JET AXIAL DISTRIBUTION ON AXIAL EVOLUTION OF C_z.

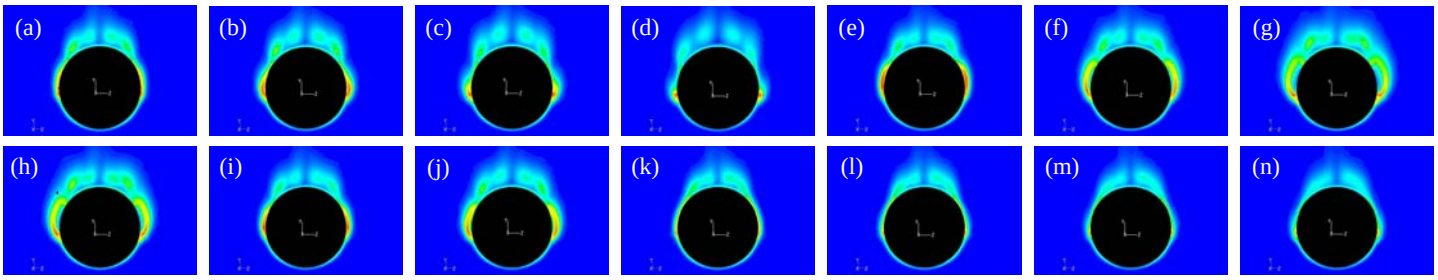

FIGURE 11. CONTOUR MAPS OF $|\omega|$ AT x/D=0.045, ALL JETS ON: (a) λ=0.30, β=60° (WINDWARD), (b) λ=0.60, β=60° (WINDWARD), (c) λ=0.90, β=60° (WINDWARD), (d) λ=1.20, β=60° (WINDWARD), (e) λ=0.30, β=120° (LEEWARD), (f) λ=0.60, β=120° (LEEWARD), (g) λ=0.90, β=120° (LEEWARD), (h) λ=1.20, β=120° (LEEWARD), (i) λ=0.30, β=120° (WINDWARD), (j) λ=0.60, β=120° (WINDWARD), (k) λ=0.30, β=0°, (l) λ=0.60, β=0°, (m) λ=0.90, β=0°, (n) λ=1.20, β=0°.

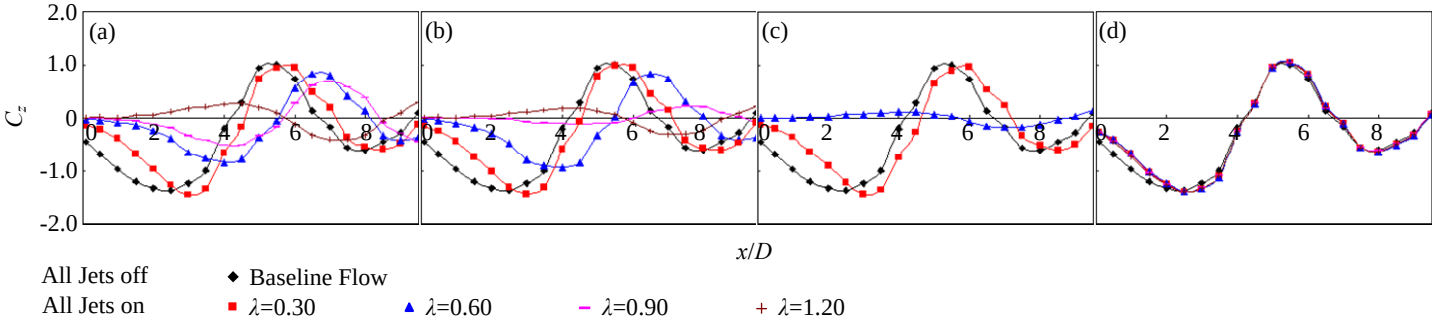

FIGURE 12. INFLUENCE OF JET-VELOCITY MAGNITUDE ON AXIAL EVOLUTION OF C_z: (a) β=60° (WINDWARD), (b) β=120° (LEEWARD), (c) β=120° (WINDWARD), (d) β=0°.

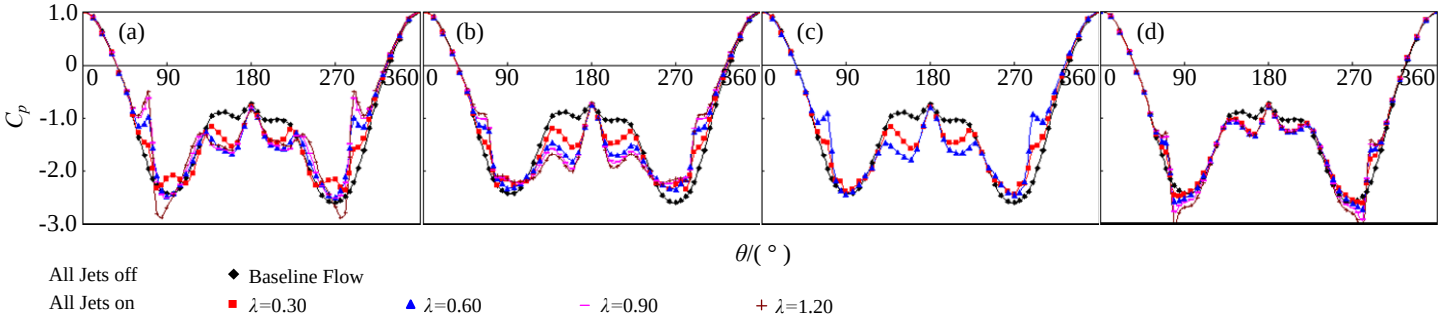

FIGURE 13. INFLUENCE OF JET-VELOCITY MAGNITUDE ON CIRCUMFERENTIAL DISTRIBUTION OF C_p AT x/D=0.045: (a) β=60° (WINDWARD), (b) β=120° (LEEWARD), (c) β=120° (WINDWARD), (d) β=0°.

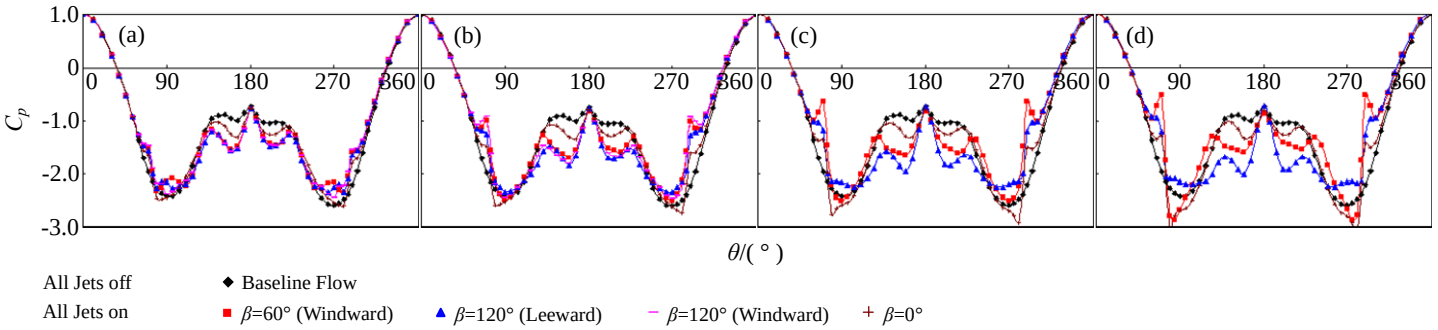

FIGURE 14. INFLUENCE OF JET SKEW ANGLE ON CIRCUMFERENTIAL DISTRIBUTION OF C_p AT x/D=0.045: (a) λ=0.30, (b) λ=0.60, (c) λ=0.90, (d) λ=1.20.

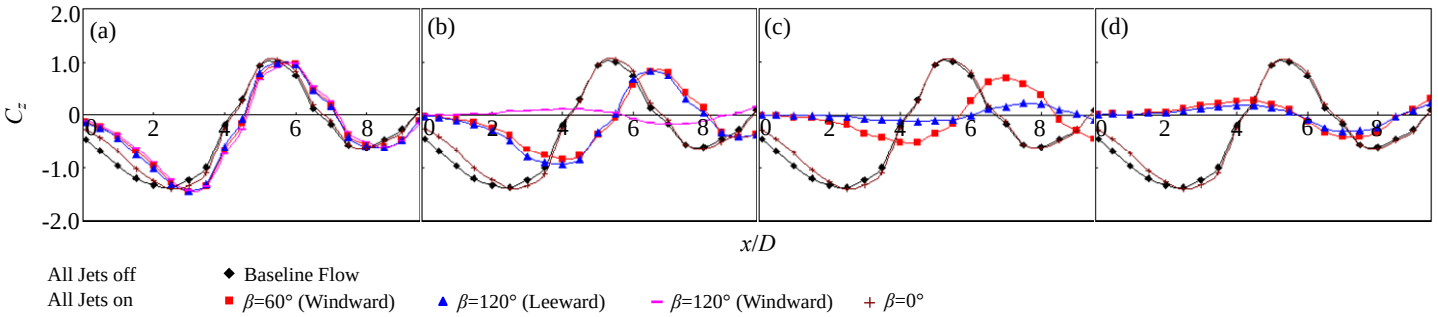

FIGURE 15. INFLUENCE OF JET SKEW ANGLE ON AXIAL EVOLUTION OF C_z: (a) λ=0.30, (b) λ=0.60, (c) λ=0.90, (d) λ=1.20.

Thus it can be seen that the strengthening of the control effect on the global flow asymmetry along with the increasing of jet-velocity magnitude is carried out through both the intensifying of concentrated vortices and the shortening of the distances between concentrated vortices and nose vortices. Well then, will the control effect strengthen infinitely along with jet-velocity magnitude increasing further? According to the above analysis, it can be inferred that with jet-velocity magnitude increasing to a certain value, the control effect will begin to weaken instead. A higher jet-velocity magnitude can bring more intensive concentrated vortices; but at the same time, it can also bring more intensive entrainment on the concentrated vortices, which will push the concentrated vortices farther away from both body surface and nose vortices. Besides, the entrainment of mainstream on concentrated vortices will strengthen when the concentrated vortices shift farther away from body surface, so the dissipation of concentrated vortices will be accelerated. It is just about these two aspects that result in the weakening of the regulation of concentrated vortices on nose vortices and further the weakening of the control effect of concentrated vortices on the global flow asymmetry.

Skew Angle of Jet Skew angle is another significant factor that influences the control effect of the minute jets on the global flow asymmetry. Under the condition of different skew angles, the intensity, shape and position of concentrated vortices are different accordingly (illustrated in Fig. 11.), and naturally their regulation on nose vortices is different (illustrated in Fig. 14.), so their control effect on the global flow asymmetry is different (illustrated in Fig. 15.).

β=0° is a special case for employing the minute jets to carry out control on the flow asymmetry, and it means that the skew directions of jets are uniform with the freestream direction. It can be clearly observed from Fig. 15. that, under such a condition, the control effect of the jets on the global flow asymmetry is always very faint and even can be neglected. The concentrated vortices originated from such minute jets are quite small, weak and always stick tightly to body surface (illustrated in Fig. 11.), which leads the concentrated vortices to stay farther away from nose vortices due to the faint entrainment of mainstream. Thus, the regulation of concentrated vortices on nose vortices is very faint (illustrated in Fig. 14.), and naturally their control effect on the global flow asymmetry is so faint.

For Jets of $\beta\neq0°$, on the premise that the jet-velocity magnitude is high enough, with skew angle altering, though the intensity, shape and position of the concentrated vortices alter, they are all intensive sufficiently and close adequately to body surface. In addition, whether the jets direct windward or leeward, the rotational directions of the concentrated vortices always keep uniform with that of the nose vortex on the same side, which assures that their partial vorticity can be convoluted into the nose vortex on the same side during the course of dissipating. That's to say, on the premise that the jet-velocity magnitude is high enough, when the skew directions are different from the freestream direction (especially when the difference is great), the concentrated vortices can strengthen, expand the nose vortices and change the shape of nose vortices, which can satisfy the requirement of performing the regulation on the asymmetry degree of the nose vortices, and lastly the effective control on the global flow asymmetry can be achieved.

All the same, under the condition of different jet skew angles, the intensity, shape and position of the concentrated vortices are different accordingly (illustrated in Fig. 11.), so their regulation details on nose vortices are different (illustrated in Fig. 14.), and naturally their control effect is different (illustrated in Fig. 15.). Well then, what is the law that the skew angle influences the control effect? It's a pity that no clear answer is achieved here, while it seems that the influence of skew angle is correlated with the jet-velocity magnitude (demonstrated in Fig. 15.).

Discussions on Control Mechanism and Optimizing Configuration of Jet Primary Parameters

Control Mechanism It has been discussed above that the control effect of the minute jets on the global flow asymmetry is realized through the direct regulation of the concentrated vortices originated from the interaction between the jets and the flow around slender body on the asymmetry degree of the nose vortices near nose apex. Well then, how do the concentrated vortices regulate the asymmetry degree of the nose vortices near nose apex?

Firstly, the concentrated vortices take inducement on the nose vortex on the same side; secondly, partial vorticity of the concentrated vortices is convoluted into the nose vortex on the same side. It can be observed from Fig. 4. and 6. that, after induced and vorticity input, the nose vortices intensify, expand and heighten. For the jets are symmetrically distributed on opposite sides, in the course of the nose vortices intensifying, expanding and heightening, the asymmetry degree of nose vortices near nose apex weakens relatively. It is obvious that, with the inducement and the vorticity transfer strengthening (for example, as the concentrated vortices intensifying and/or their distances away from nose vortices shortening), the asymmetry degree of nose vortices near nose apex weakens further.

So based on the conclusion about the correlation between the asymmetry degree near nose apex and the global flow asymmetry drawn from Ref. [7], as the asymmetry degree of nose vortices near nose apex is regulated by concentrated vortices, naturally the flows of different asymmetry degrees can be achieved (i.e., the active control can be achieved).

Rules on Optimizing Configuration of Jet Primary Parameters For the control effect of the minute jets on the global flow asymmetry is realized through the regulation of concentrated vortices on the asymmetry degree of nose vortices near nose apex, several requests for achieving the effective regulation should be cleared firstly. Based on the above discussion, three primary factors are supposed to be responsible for the regulation: intensity of concentrated vortices, distances between concentrated vortices and nose vortices, axial extent of concentrated vortices keeping acting on nose vortices. In other words, the active control is realized through adjusting these three factors by directly configuring the jet primary parameters. However, no matter how to configure the jet primary parameters (including both those discussed above and never discussed in the current work, such as caliber, circumferential distribution, pitching angle, etc.), for achieving the effective regulation and further the control effect on the global flow asymmetry, the next three rules should be followed.

(1) The concentrated vortices are intensive sufficiently, for this is the basic of the control effect. The more intensive the concentrated vortices are, the more intensive the regulation is, and further the more intensive the control effect is.

(2) The concentrated vortices are close enough to nose vortices when forming, for concentrated vortices dissipate rapidly downstream. If the distances are too long, no matter how intensive the concentrated vortices are, the regulation must be extremely faint. The shorter the distances are, the more intensive the regulation is, and further the more intensive the control effect is.

(3) The concentrated vortices keep acting on nose vortices in an adequately long axial extent. Since the concentrated vortices dissipate rapidly after forming, the axial extent of a single pair of jets acting on nose vortices is quite limited, and accordingly the restraint on the development of the flow asymmetry near nose apex is momently. Therefore, it is necessary to adopt at least two pairs of jets distributed axially in reason to effectively delay the axial position of obviously asymmetric pattern beginning to appear.

CONCLUSIONS

An active method with minute jets distributed symmetrically on opposite sides before separation lines near nose apex is advanced to control the flow asymmetry around slender body of revolution at high incidence. By numerically discussing the control effects under different configurations of jet primary parameters, several conclusions are achieved.

(1) The control effect is realized with the concentrated vortices originated from the interaction between the jets and the flow around slender body. With concentrated vortices inducing and providing nose vortices with vorticity, the asymmetry degree of nose vortices near nose apex is regulated, and further the global flow asymmetry is controlled actively.

(2) The control ability lies on the regulation intensity of concentrated vortices on nose vortices, which is primarily influenced by three factors: intensity of concentrated vortices, distances between concentrated vortices and nose vortices, axial extent of concentrated vortices keeping acting on nose vortices. The active control can be achieved by directly configuring the jet primary parameters to adjust these three factors. When configuring parameters, the next three rules should be followed: (a) concentrated vortices are intensive sufficiently; (b) concentrated vortices are close enough to nose vortices; (c) concentrated vortices keep acting on nose vortices in an adequately long axial extent, which requires the cooperation of at least two pairs of jets distributed axially.

ACKNOWLEDGMENTS

Thank the peer Reviewers for their valuable suggestions. Thank the colleagues in both Lab for Advanced Simulation of Turbulence, School of Aerospace, Tsinghua University and 105 Research Lab, School of Mechanical Engineering, Nanjing University of Science and Technology, for their help in discussion and text proofreading.

REFERENCES

[1] Allen, H. J., Perkins, E. W., 1951, “Characteristics of Flow over Inclined Bodies of Revolution,” NACA RMA50L07.

[2] Thomson, K. D., Morrison, D. F., 1971, “The Spacing, Position and Strength of Vortices in the Wake of Slender Cylindrical Bodies at Large Incidence,” J. Fluid Mech., 50(4), pp. 751-783.

[3] Hunt, B. L., 1982, “Asymmetric Vortex Forces and Wakes on Slender Bodies,” AIAA Paper No. 1982-1336.

[4] Ericsson, L. E., Reding, J. P., 1985, “Aerodynamic Effects of Asymmetric Vortex Shedding from Slender Bodies,” AIAA Paper No. 1985-1797.

[5] Wang, G., Deng, X. Y., Wang, Y. K., Chen, X. R., 2003, “Zonal Study of Flow Patterns around an Ogive-Cylinder at Subcritical Reynolds Numbers,” Exp. Meas. Fluid Mech., 17(2), pp. 19-25+36.

[6] Keener, E. R., Chapman, G. T., Kruse, R. L., 1976, “Effects of Mach Number and Afterbody Length on Aerodynamic Side Forces at Zero Sideslip on Symmetric Bodies at High Angles of Attack,” AIAA Paper No. 1976-0066.

[7] Guan, X. R., Xu, C., Wang, Y. J., Wang, Y. P., 2009, “Influence of Nose-Perturbation Location on Behavior of Vortical Flow around Slender Body at High Incidence,” Sci. China Ser. E - Tech. Sci., 52(7), pp. 1933-1946.

[8] Moskovitz, C. A., Dejarnette, F. R., Hall, R. M., 1989, “Effects of Nose Bluntness, Roughness and Surface Perturbations on the Asymmetric Flow past Slender Bodies at Large Angles of Attack,” AIAA Paper No. 1989-2236.
[9] Degani, D., 1990, “Numerical Investigation of the Origin of Vortex Asymmetry,” AIAA Paper No. 1990-0593.
[10] Bernhardt, J. E., Williams, D. R., 1998, “Proportional Control of Asymmetric Forebody Vortices,” AIAA J., 36(11), pp. 2087-2093.
[11] Wang, G., Liang, X. G., Deng, X. Y., 2004, “Effects of Roll Angle on Side Force Distribution over Slender Bodies of Revolution at High Angle of Attack,” Exp. Meas. Fluid Mech., 18(4), pp. 11-14.
[12] Liu, P. Q., Wang, G., Deng, X. Y., 2003, “Experimental Study of Reynolds Numbers Effect on Asymmetric Vortices and Their Aerodynamic Characteristics over a Slender Body,” Exp. Meas. Fluid Mech., 17(4), pp. 10-16.
[13] Deng, X. Y., Wang, Y. K., Chen, X. R., 2003, “Deterministic Flow Field and Flow Structure Model of Asymmetric Vortices over Slender Body,” AIAA Paper No. 2003-5475.
[14] Calarese, W., 1981, “An Experimental Study of Vortex Flow in the Wake of a Slender Body of Revolution at Large Incidence,” AIAA Paper No. 1981-0359.
[15] Lamont, P. J., 1982, “The Complex Asymmetric Flow over a 3.5D Ogive Nose and Cylindrical Afterbody at High Angles of Attack,” AIAA Paper No. 1982-0053.
[16] Keener, E. R., Chapman, G. T., 1977, “Similarity in Vortex Asymmetries over Slender Bodies and Wings,” AIAA J., 15(9), pp. 1370-1372.
[17] Moskovitz, C. A., Dejarnette, F. R., Hall, R. M., 1991, “New Device for Controlling Asymmetric Flowfields on Forebodies at Large Alpha,” J. Aircr., 28(7), pp. 456-462.
[18] Ericsson, L. E., Reding, J. P., 1980, “Alleviation of Vortex-Induced Asymmetric Loads,” J. Spacecr. Rockets, 17(6), pp. 546-553.
[19] Chen, N. Q., Wang, Z. Y., Huang, Z., 1997, “Asymmetric Vortices and Alleviation on Slender Bodies with and without Wings,” AIAA Paper No. 1997-0748.
[20] Rao, D. M., 1979, “Side-Force Alleviation on Slender, Pointed Forebodies at High Angles of Attack,” J. Aircr., 16(11), pp. 763-768.
[21] Williams, D. R., 1997, “A Review of Forebody Vortex Control Scenarios,” AIAA Paper No. 1997-1967.
[22] Pedreiro, N., Rock, S. M., Celik, Z. Z., Roberts, L., 1996, “Roll-Yaw Control at High Angle of Attack by Forebody Tangential Blowing,” AIAA Paper No. 1996-0773.
[23] Roos, F. W., 1998, “Synthetic-Jet Microblowing for Forebody Flow-Asymmetry Management,” AIAA Paper No. 1998-0212.
[24] Rao, D. M., Murri, D. G., Moskovitz, C., 1987, “Forebody Vortex Management for Yaw Control at High Angles of Attack,” J. Aircr., 24(4), pp. 248-254.
[25] Murri, D. G., Shah, G. H., Dicarlo, D. J., Trilling, T. W., 1995, “Actuated Forebody Strake Controls for the F-18 High-Alpha Research Vehicle,” J. Aircr., 32(3), pp. 555-562.
[26] Viviand, H., 1974, “Conservative Forms of Gas Dynamics Equations,” La Recherche Aerospatiale, (1), pp. 65-68.
[27] Menter, F. R., 1994, “Two-Equation Eddy-Viscosity Turbulence Models for Engineering Applications,” AIAA J., 32(8), pp. 1598-1605.
[28] Roos, F. W., Magness, C. L., 1993, “Bluntness and Blowing for Flowfield Asymmetry Control on Slender Forebodies,” AIAA Paper No.1993-3409.
[29] Ng, T. T., Malcolm, G. N., 1991, “Aerodynamic Control Using Forebody Blowing and Suction,” AIAA Paper No. 1991-0619.
[30] Hwang, S. J., Rho, O. H., 1995, “Numerical Simulation of Asymmetric Vortical Flows on a Slender Body at High Incidence,” AIAA Paper No. 1995-1799.
[31] Guan, X. R., Xu, C., 2009, “Numerical Investigation of Boundary-Layer Control Using Minute Jet Vortex Generator,” Eng. Mech., 26(4), pp. 214-220+245.
[32] Levy, Y., Degani, D., Seginer, A., 1990, “Graphical Visualization of Vortical Flows by Means of Helicity,” AIAA J., 28(8), pp. 1347-1352.